Quasar Spectrum Analysis

Victoria Tielebein – Gordon Richards

Submitted in partial fulfillment of the requirements for the degree of Bachelor of Science in Physics

Drexel University, Philadelphia, PA, 16 May 2014

Contents

Abstract

Quasars are highly luminous and dense galactic nuclei with anisotropic radiation patterns. The current structural model of a quasar places a super massive black hole at the center of an accretion disk so luminous that it outshines the entire rest of the galaxy. A donut-shaped region called the “torus” forms thick, nearly opaque clouds of dust from wind off of the accretion disk, obscuring interior quasar radiation from view at certain angles. For this reason, observational data providing the basis of quasar physics may be biased or incomplete. However, a theory called the “clumpy model” proposes discrete cloud alignment along magnetic field lines. This model implies a reality in which some radiation escapes from the interior of the quasar even through the torus, allowing for increased capacity to study AGN physics. If this model were correct, anomalies would likely exist in spectral comparisons of time separated quasar measurements. The Sloan Digital Sky Survey (SDSS) now has a large enough collection of quasar spectra to facilitate the search for this type of observational evidence. For this purpose, software will be developed to download and determine “matches,” i.e. multiple spectra taken for the same celestial object, plot these matches in one window, and adjust these plots for analysis. While the cause of many such anomalies is likely calibration differences or atmospheric effects, some of the more unique anomalies may indicate support for the clumpy model and other known structural aspects of the quasar standard model.

Introduction

Quasars are the light bulbs of the universe. Highly luminous and energetic cosmic bodies, these powerful engines convert matter into electromagnetic energy on huge galactic scales. Quasars likely play a major role in the evolution and formation of our universe, but studying them is not trivial. With so much still to learn, it is crucial to optimize methods of viewing and measurement techniques for these incredible celestial objects.

Section I - Summary of Relevant Quasar Structure

Quasi-stellar radio sources, or "quasars," are Active Galactic Nuclei (AGN), meaning that they are the center points for galaxies and are accreting. Galaxy structure directly determines how much radiation quasars can produce, therefore also determining quasar luminosities; elliptical galaxies tend to produce the most luminous quasars (further explanation: Fanidakis 2013, and see Section III). Quasars are among the most luminous objects in the universe, and yet they appear amongst the faintest objects in the night sky on Earth because of how far away they are on average. This vast distance further implies that light from these objects has taken a very long time to reach Earth. In fact, observed quasars have co-moving distances ranging from 600 million to 28.85 billion light years (redshifts observed between 0.056 and 7.085) (Urry 1995). This means that some of the farthest observable quasars are extraordinarily young galaxies.

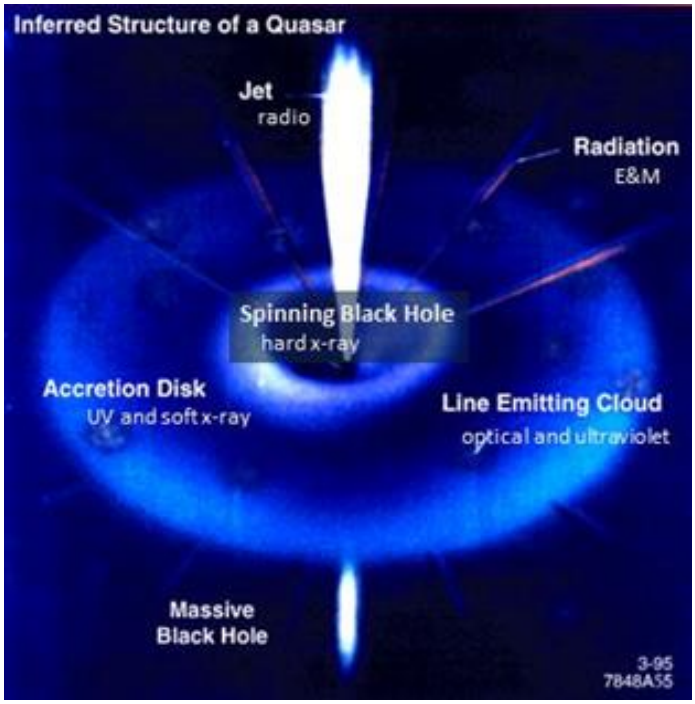

Figure 1
Above shows the various regions of a quasar (from the "broad-line cloud model") with the type of radiation they

Quasars are like generators in that they use "fuel" to produce vast amounts of energy. This process begins when excess matter (the fuel) enters a black hole's strong gravitational pull. The matter alters path slightly as it falls inward, following a tendex, or spiral-shaped, line. The extreme gravitational gradient surrounding a black hole causes the matter to fall at different rates, intensifying frictional forces and significantly increasing temperature. This excess energy is then released as electromagnetic radiation (further reading: Floyd 2009). However, only a small fraction of a quasar's total mass is emitted in this way (an amount still estimated to be greater than 10x that of solar fusion). The excess matter fueling this accretion is often known as a "bulge" (for details on how bulge properties relate to quasar behavior, see: Fanidakis 2013), and is theorized to accumulate from a number of sources. One such source could be a binary star system, in which it is common for the larger star to collapse first, typically in a Type IA Supernovae. This explosion forms a black hole of much higher density which often begins absorbing the smaller star in

steady, continuous increments. This type of black hole is an excellent candidate for accretion, although it would make a rather weak quasar (and in fact would likely never be recognized as a quasar) (further reading: Shakura 1973). This is because the amount of energy required to power a scaled-to-universe-sized light bulb is immense. These types of quasars typically only form around **supermassive** black holes and require a trigger far more extreme than the death of a star. One such trigger could be the merging of two galaxies (further reading: Neistein 2013). In fact, it's possible that our own Milky Way galaxy could once have been a quasar like these (formed from collisions of smaller galaxies), or that it may yet become one (albeit a weak one) when it merges with Andromeda. There is compelling reason for either or both of these scenarios to be the case; quasars exist across a large range of redshifts and comprise only a small percentage of the total known galaxies, clearly implying a dynamic role in the formation and evolution of galaxies. These engines will eventually run out of fuel and shut down (Thomsen 1987). Without their accretion, the light bulb turns off and the host galaxy can be seen more distinctly.

Each component of a quasar produces electromagnetic radiation of some type. The accretion disk radiates energy in the ultraviolet and soft x-ray range. Hard x-ray lines are produced by the spinning of the black hole itself (Urry 1995). Occasionally, energetic particles which gather up near the poles of the torus escape in collimated radio-emitting jets. The plasma in these jets shoots out at an extremely high velocity, beaming radiation into space at relativistic speeds (Blandford 1974, Urry 1995). A visual model of these observations is included in Figure 1.

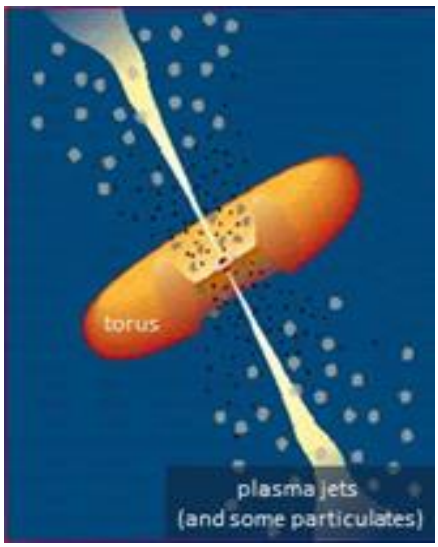

Figure 2
Above shows the torus as a perfect, opaque tube. In the clumpy model, the shape would be roughly the same, but the clouds would be drawn more discretely.

The "disk-wind" model of quasars is a theory in which wind off of the accretion disk blows some of the material contained within further out into space (originally proposed here: Murray 1995). However, because of the high gravity of the black hole center, the wind doesn't disperse. Instead, because there is less turbulence farther out, stray accretion disk particles accumulate and experience organic chemistry in this region, forming dust. This region of "dusty clouds" is called the "torus." The torus encircles the accretion disk and obscures the interior of the quasar from being viewed by certain angles. Figure 2 is a rough representation of the torus region (further reading: Urry 1995).

One of the original features quasars were thought to possess included a "broad-line cloud" region (refer back to Figure 1), where winds off of the accretion disc produced strong optical and UV emission lines. While this is still a possibility, more recent research has indicated that these "broad-line clouds" are actually an inner layer of the torus itself. In this model (proposed and further explained here: Nenkova 2008), the inner clouds of the torus lie within the dust sublimation radius, and so are too turbulent for dust to form. Instead, direct exposure to internal AGN radiation causes the particles here to ionize, producing broad line spectrum emissions. The lack of dust in this inner region implies the absorption of X-ray radiation only, while optical and UV radiation would largely traverse this region intact. The outer

clouds are shielded from all of the ionizing radiation by the inner cloud region, allowing for the formation of optically thick clouds of dust. Optical and UV radiation from the accretion disk would therefore be absorbed by this outer region and re-radiated as infrared radiation (Nenkova 2008).

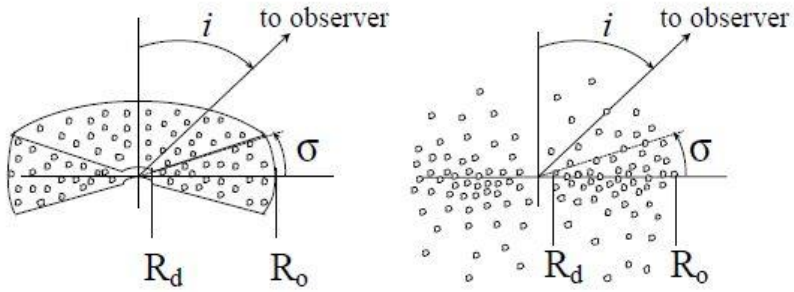

Figure 3
In this diagram, the torus is displayed as a cross-section comprised of packets of discrete, "clumpy" clouds. In both diagrams, the inner radius is that of dust sublimation and is represented by $\mathbf{R_d}$. The outer radius is $\mathbf{R_0}$. On the left, the angular distribution has a sharp-edge, and on the right, a smooth boundary (i.e. Gaussian). For full explanation of these models, and their derivations, please see (Nenkova 2008).

This model, a theory describing "clumpy" tori, was originally constructed to remedy the discrepancy between observational and predictive behavior of silicate absorption lines (described here: Nenkova 2002). A diagram depicting a clumpy torus is shown in Figure 3. However, the vast implications of such a model are clear, and many of the known structural features of quasars have been modified in response (as described to some extent above). The model essentially states that torus clouds are not continuously distributed, but rather form into discrete clumps (perhaps along magnetic field lines). This means that the probability of viewing the AGN through the optically thick and dusty clouds of the outer torus is small, but non-zero (Nenkova 2008). So in theory, some of the aforementioned optical and UV radiation normally absorbed by the outer torus clouds should appear as anomalies in comparisons of time-separated AGN spectral measurements. Standardly anomalous data will surely exist due to the large number of possible measurement and machine errors, not to mention the effect which atmospheric or other physical conditions may have had. However, if considerations are made for some of the more obvious factors, then it would certainly be reasonable to expect that a handful of significantly anomalous spectral comparisons exist. Finding zero anomalies in a data set this large would certainly also be significant. Further discussion on this can be found in Sections VII and VIII.

Section II – Introduction to Astronomical Spectroscopy

A spectrum is a plot of light intensity (or flux) versus light wavelength, essentially showing the full picture of an object including the parts of the electromagnetic spectrum that are not visible to the human eye. Black bodies are objects which perfectly absorb light at every wavelength and whose spectra are nearly perfect parabolic shapes, with the peak reflecting the temperature of the object alone. From a straight-line view, this would appear as a continuum, as shown in Figure 4. If something like gas were placed in between the object and observer, then the viewing angle would determine the shape of the spectrum. An absorption spectrum shows what wavelengths of light the gas absorbs and an emission spectrum shows what wavelengths of light are scattered. These two spectra indicate what type of material the gaseous cloud contains. Each type of celestial body has a different characteristic

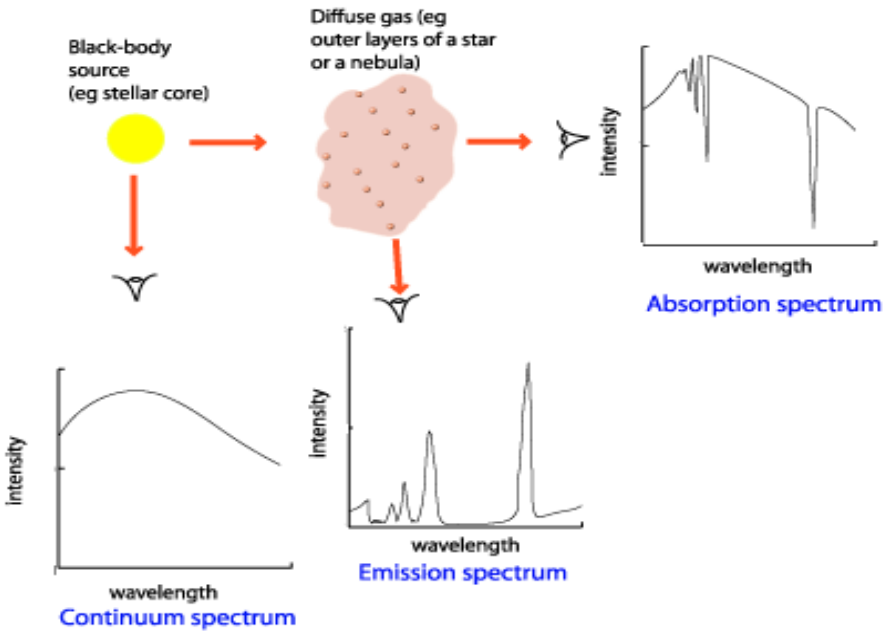

Figure 4

Spectra appear differently depending on how they are viewed. A continuum means direct line-of-site. Emission and Absorption spectra are created when light passes through a cloud of gas, during which certain wavelengths of light are scattered or absorbed respectively. The viewing angle determines which of these features appear.

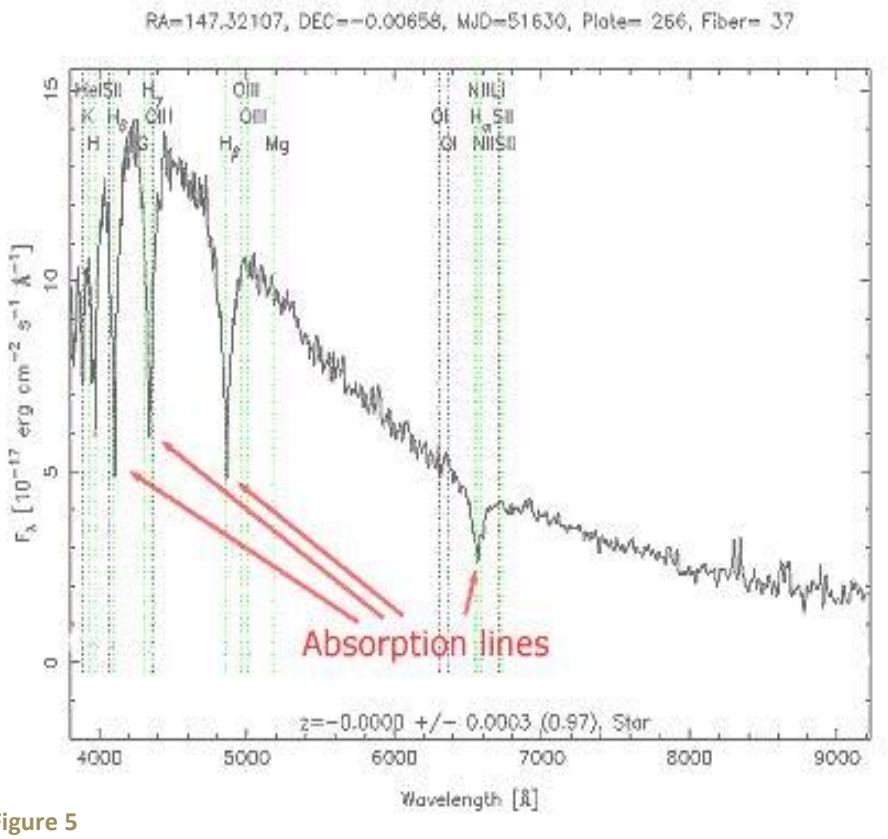

Figure 5

A star spectrum with the characteristic peak. This particular star is fairly hot, and its absorption lines indicate the atomic make of its core and atmosphere.

spectrum. The spectra for any two different objects will never be identical even if they are the same type of object or have similar atomic make, especially given the impact which natural obstructions in space may have on the measurements.

Star spectra (see Figure 5) look remarkably like black body spectra, with the occasional absorption line detailing the chemical make-up of the star's core and atmosphere. Where the peak lies on the spectrum refers to the temperature of the star, with shorter wavelengths indicating higher temperatures. Galaxy spectra (see Figure 6) are summations of all of the light of all of the stars they contain. Since hot stars burn much brighter and faster than cool stars, galaxy spectra typically maintain a star-like parabolic shape, but with a less pronounced peak that is shifted more toward the center. This makes sense since galaxies essentially represent the average of many hot, short-lived stars plus many, many more, cool and long-lived stars. The rough, jagged shape of a galaxy spectrum comes from the vast amount of gas contained amongst the stars, as well as the galaxy's redshift ("Types of Astronomical Spectra").

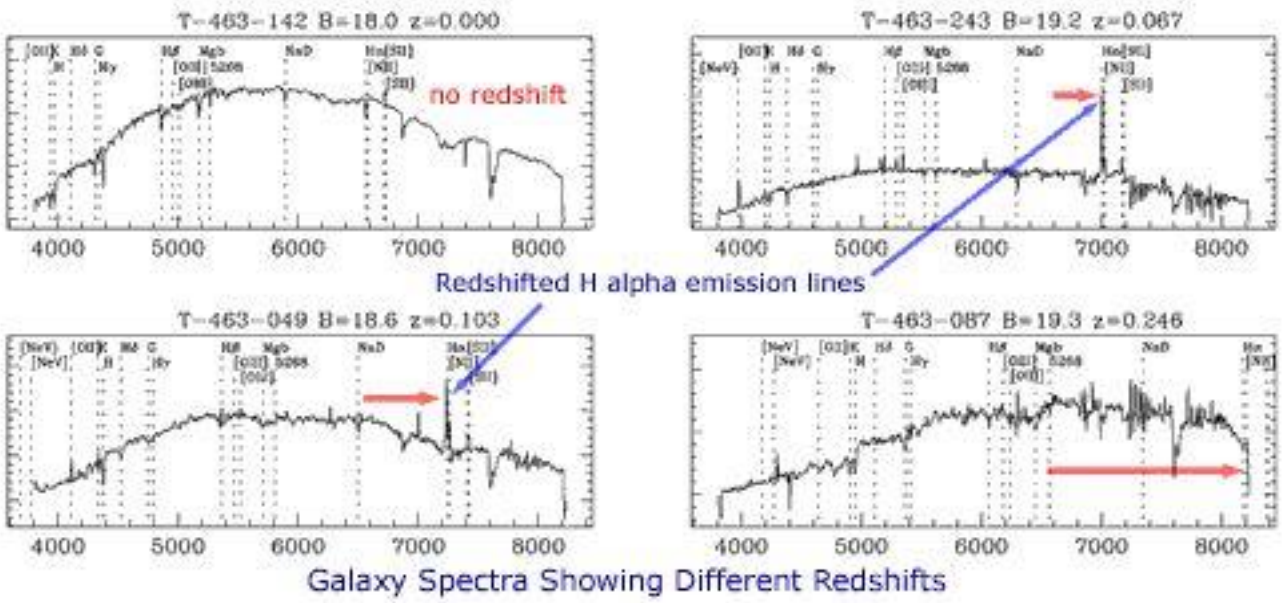

Figure 6

Above are four galaxy spectra. Notice the characteristic parabolic shape near the center of the X axis and the handful of absorption lines indicating gas composition. This particular diagram also illustrates the effect that redshift has on spectra: increasing z values for redshift correspond with shifted emission lines toward the redder end of the spectrum.

Quasar spectra are a lot more complicated and interesting than other celestial spectra. Quasars are essentially just galaxies, but with large and highly luminous accretion disks (which more often than not, outshine the entire galaxy). Therefore, one might expect that a quasar spectrum would look roughly the same as a galaxy, but with large peaks at particular, characteristic wavelengths which tend to dwarf the rest of the spectrum with their amplitudes. This guess wouldn't be too far from the truth, but it's worth noting the variation amongst different AGN spectra, which often appear to be quite odd and seemingly counterintuitive. This is because there are several different classifications of AGN, and each has its own characteristics. Initially, each classification was believed to be a different celestial object; however, unification attempts have proven quite successful in demonstrating that each type is a reflection of the same phenomenon from different viewing angles and under different evolutionary stages. The foundation and most extensive explanation of unification attempts can be found in (Urry and Podovani 1995), with some of the more relevant bits summarized below.

Section III - High-Level Overview of AGN Classifications

AGN are categorized according to several traits: their radio loudness, the broadness of their emission lines, and the relative strength and peculiarity of their line emissions, if they have any. Throughout this discussion, please refer to Figure 7 for a graphical representation of the different classifications, provided by (Urry and Podovani 1995).

Type 1 AGN are those with bright continua and broad emission lines, resulting from hot, high-velocity gas presumed to exist close to their black holes' potential. A radio-quiet example from this category is the Seyfert 1 galaxy, a type which is typically fairly dim (such that the host galaxy can often be resolved) and therefore only observable at small redshifts. Quasars (QSOs) are the higher-luminosity, radio-quiet AGNs labeled Type 1. These are less common, can only be seen at great distances, and are typically so

bright that the host galaxy is completely obscured from view. A radio-loud, Type 1 AGN could be considered a Broad-Line Radio Galaxy, Steep Spectrum Radio Quasar, or Flat Spectrum Radio Quasar, depending on the shape of its radio continuum (Urry and Podovani 1995).

TABLE 1
AGN Taxonomy
Optical Emission Line Properties

Radio Loudness	Type 2 (Narrow Line)	Type 1 (Broad Line)	Type 0 (Unusual)
Radio-quiet:	Sy 2	Sy 1	
	NELG		
	IR Quasar?	QSO	BAL QSO?
Radio-loud:	NLRG {FR I, FR II}	BLRG, SSRQ, FSRQ	Blazars {BL Lac Objects, (FSRQ)}

Black Hole Spin? ↓

Decreasing angle to line of sight →

Figure 8
Table from (Urry and Podovani 1995) illustrating the different AGN Classifications with examples from each type. Those closer to this captions are more luminous, which is now understood to correspond with black hole mass.

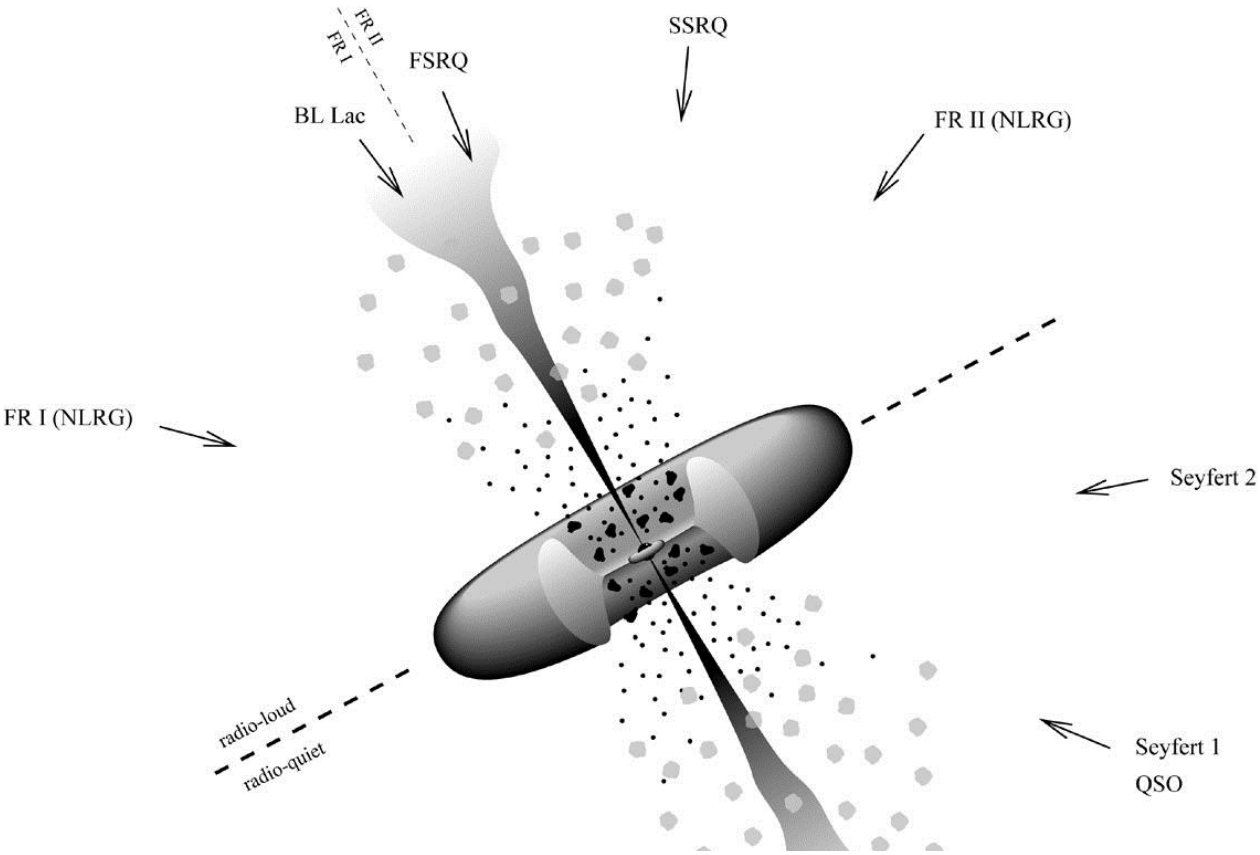

Figure 7
According to widely accepted unification theories, each different type of known quasar spectra actually describes the same physical phenomenon (accretion from AGN), but from different viewing angles. This is sometimes referred to as the "standard model of quasars."

Type 2 AGN have weak continua and only narrow emission lines, implying one of two things: either the accretion disk is comprised of cool, low-velocity gas, or the direct line of sight is obscured by thick, toroidal clouds. An example of a radio-quiet, Type 2 AGN is the Seyfert 2 galaxy, producing rather low luminosities. Radio-loud, Type 2 AGN include two distinct morphologies: those with low-luminosity, symmetric radio jets, which decrease in intensity and fall away from the nucleus; or those with high-luminosity, highly collimated radio jets, possessing well-defined lobes and prominent hot spots. These are called Fanaroff-Riley Type I or II galaxies, respectively (Urry and Podovani 1995).

A small number of AGN are particularly odd, and are occasionally referred to as Type 0 AGN. This classification includes BL Lacertae objects, which are radio-loud AGN with almost no absorption or emission features, and Broad Absorption Line (BAL) quasars, which are radio-quiet and possess unusually broad P-Cygni-like absorption features in the optical and ultraviolet range. Classifying AGN with similarly bizarre spectral behavior is certainly a challenge and subject to much debate within the field today (Urry and Podovani 1995). However, disputes about AGN classification are decreasingly significant as the prevalence of unification schemes rises.

Conjectures about the impact of galaxy type and black hole behavior on radio-loudness, which were founded in the late 1980s, have seen great support from recent research. Roughly 15 – 20% of AGNs are radio-loud, signifying a radio to optical flux ratio larger than about 10 (Urry and Padovani 1995). Radio-loudness is inversely proportional to the Eddington ratio, and so therefore correlated with large black hole masses (Sikora 2007). Furthermore, similarities which radio-loud and radio-quiet AGN share in the optical and ultraviolet emission-line spectra and the infrared to soft X-ray continuum imply that a significant portion of spectral data must be produced by essentially the same means regardless of radio-loudness (Urry and Podovani 1995). Results like these are substantial in demonstrating that AGN stem from the same physical phenomenon, but take different forms based on viewing angle, time evolution, galaxy type, and other similar conditions. This unification scheme, sometimes referred to as the "standard model of quasars" is illustrated in Figure 8.

Section IV – Spectrum Analysis Methods

If the clumpy theory were correct, then anomalies would likely appear in spectral comparisons of time separated quasar measurements, henceforth referred to simply as "comparisons." These comparisons indicate in-depth analysis of the similarities and differences between 2 or more different spectra recorded for the same

Figure 9
This shows the rough layout of the plotting UI for a comparison.

quasar object at different Mean Julian Dates (MJDs). Figure 9 shows an example comparison. Spectra are considered matches if the angular distance between their spherical coordinates is less than 2 arcseconds as determined thusly:

$$r_n = RA_n \times \cos(Dec_n)\text{ , and}$$

$$l = \sqrt{(r_1 - r_2)^2 + (Dec_1 - Dec_2)^2} \times 3600\ arcseconds\text{ ,}$$

where *RA* and *Dec* are the coordinates of each object and $l \leq 2$ implies a match.

The nature of expected anomalies is not yet definitive, but should incorporate the known features of quasar structure described in the previous sections. To start off, comparisons which show a distinct change in UV or optical radiation levels will be considered significant. Changes like this may result from a probabilistic, yet discrete torus. However, due to the generally anisotropic nature of quasars, more specific criteria will have to be determined before conclusions can be drawn. Comparison analysis will be conducted manually using a new spectrum analysis tool described in the next section.

Section V - Development of Spectrum Analysis Application

In order to conduct this research, software with unique functionality needed to be developed. This application is a tool for astronomy researchers in various fields. Included are several straight-forward UIs with functionality for downloading and comparing massive amounts of spectral data at once. The user inputs key SDSS fit file information such as the right ascension, declination, MJD (mean Julian date), plate, or fiber number for a particular object. This information then sorts a list of local fit files to display only those relevant to the user input. This list can also be limited to display only spectra with known

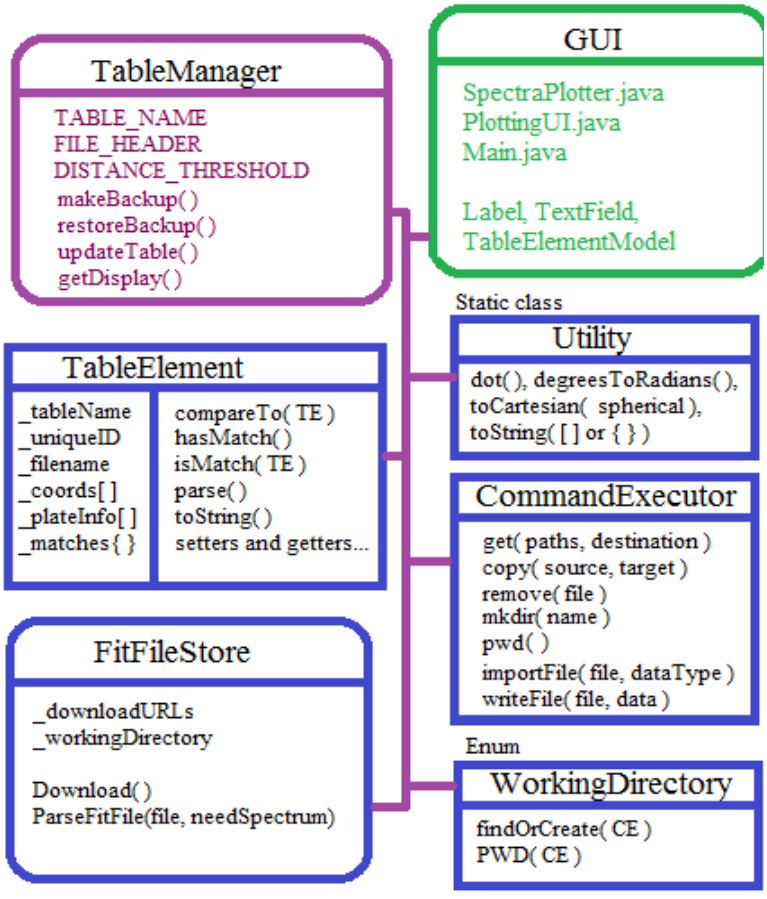

Figure 10
Above shows a rough diagram of the application.

matches. If no files exist locally with the inputted information, then they can be downloaded easily. All the user must supply to download a particular plate is the MJD and plate number. If only one file is needed, then the user may specify a fiber number as well so that only that particular file is retrieved. For convenience, a list of this information can be uploaded as well so that each file need not be individually specified. Downloaded files are compared against other local copies and match information is stored.

Files that exist locally can be plotted using the spectra plotting tool. If there are multiple spectra for a single object, then the plotter will automatically display all of these in the same window. If only two spectra are selected, then the plotter will also display their ratio. Selection of which spectra to plot at once for the same object can be modified in the plot options menu. Other plot functionality includes zoom and panning features, smoothing options, and axis adjustment. The plotter also allows the user to quickly flip through data by skipping to the next or previous comparison in the list, automatically applying the user's current plot options in the next display frame as well. Please refer back to Figure 9 for the rough layout of this plotting interface (some features may be different as updates are ongoing).

Figure 10 shows the class structure of the software in more detail, including most function names and parameters. The software is primarily expected to analyze many quasars at a casual pace, having thus been optimized for this purpose. Construction on the software will continue, and user feedback will be incorporated in the development of new features. A framework for this continued effort will be set-up and announced separately. As the SDSS database grows, so too can this local spectra database very naturally and with little required maintenance. Relevant and interesting excerpts of code can be found in Appendix I and the documentation in Appendix II.

Notes on software design choices:

- Java was selected for its extreme versatility, easy portability, and built-in data handling.
- Match information storage is not intensive, so SQL added needless complexity. Instead, a text file suffices, using the made-up extension "qst" ("quantum spectra table") for disambiguation.
- The determination of matches involves the calculation of angular distance between objects. There are other header values which could be used to optimize the accuracy of match detection, which later programmers can explore and incorporate fairly easily within this framework. The math calculation is contained within "TableElement.java," and is shown in Appendix I.

Section VI - Data

The Sloan Digital Sky Survey (SDSS) contains spectra for over 150 thousand known quasars, a sample finally large enough to facilitate this type of research. The SDSS telescope is 2.5 meters in diameter and located at Apache Point Observatory in New Mexico. Quasar spectra have been accumulated throughout 3 different surveys and several different data releases, in many instances creating multiple spectrum files for each quasar object (a.k.a. "matches").

SDSS I & II were performed with a CCD camera, obtaining results in 5 optical bands. SDSS III used 30, 2048x2048 pixel CCDs, covering over 14,500 unique square degrees of sky. Full reference of spectrum

analysis and catalogue details can be found in (Stoughton 2002, Schneider 2010, and Paris 2012) respectively. Objects were calibrated both photometrically and astrometrically in all three surveys, however some major improvements were made to the spectroscopic equipment between the earlier and later data releases, including: correction to the instability of spectroscopic flats, improved wavelength and spectrophotometric calibration, improved SEGUE Stellar Parameter Pipeline, and more efficient and less error prone handling of strong, unresolved emission features (Abazajian 2009). Controls for the improved equipment, as well as varying atmospheric conditions on different observation days, will be considered in determining comparison anomaly criteria.

The SDSS telescope determines which objects to observe on any given night by a system of large metal plates with holes, known as "fibers," drilled into them. The fibers allow only that light which corresponds to certain coordinates on the night sky to pass through into the telescope, limiting the number of objects observed at any given time for better quality measurements. Spectra taken from different fibers on the same plate cannot possibly be duplicates since the minimum drilling distance for fibers is 55 arcseconds and spectra are only considered matches if they lie within 2 arcseconds of one another. However, the same plate is occasionally used multiple times (assigning each with a different MJD), producing matches. Plates are perfectly circular and so must overlap in order to cover the entire night sky, producing yet more matches.

The three unique sources for spectra matches together produce more than enough data for comparison analysis. If there are substantial matches within each data release, then such factors as improved equipment and spectroscopy techniques will require less consideration. Likewise, a data set like this allows for cross-referencing anomalies found within data releases to those found across releases, indicating the type of impact improved equipment has in general. This could potentially be used to create a maintainable comparison algorithm and automate the analysis process for years to come.

Section VII - Results

SDSS plates are not organized by object type, so first and foremost, analysis requires distinguishing between galaxies, quasars, and stars, an explanation of which is found above in Section III. Throughout this analysis, spectra type will be specified and in some instances examined.

As expected, anomalies are many times identifiable as calibration errors. The top comparison in Figure 11 shows one such instance (matching spectra are 55831-5146-84 and 55854-5147- 455). When one spectra has more flux than the other at every point within one optical filter (also known as bands), while the general shapes of both spectra are the same, then there is likely something off with the calibration for that particular filter. The SDSS knows a great deal about the source of such calibration issues, although software like this one does bring to light the exact nature of the problem more clearly (Abazajian 2009 and Paris 2012).

Another unsurprising, albeit less common, source of anomalies comes from atmospheric conditions on earth during the time of measurement. Because the SDSS array is located in NM, weather conditions are

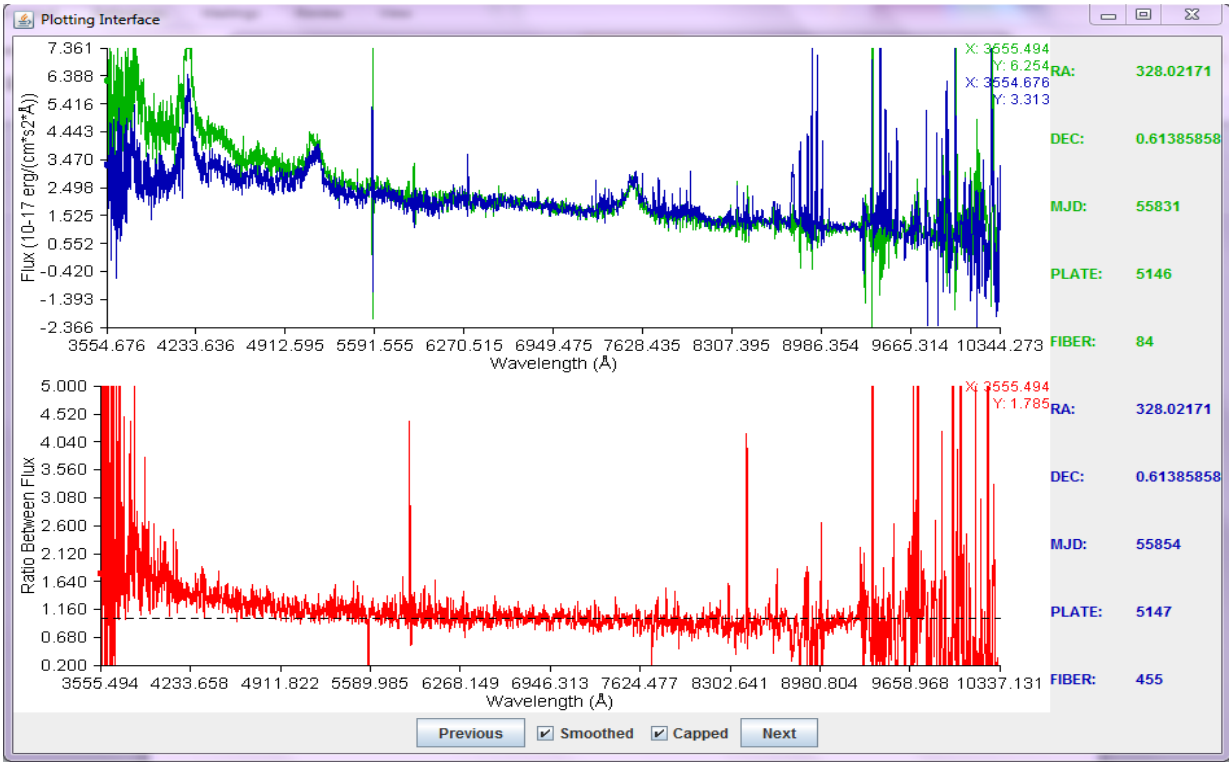

Figure 11

Above (quasar) depicts a likely example of calibration error since one spectrum has greater flux than the other throughout the entire U band (and just this band). Below is less certain; it's possible that these are standard galaxy spectra and earth's atmospheric conditions absorbed much of the flux from one and not the other (say if it was a little cloudy). However, there is an odd feature for galaxies present in both spectra: a prominent peak around 7350 Å, almost exactly where the Hβ line would be in a quasar. This feature may indicate a transition for this galaxy, during which may either be turning on (and becoming a quasar), or turning off.

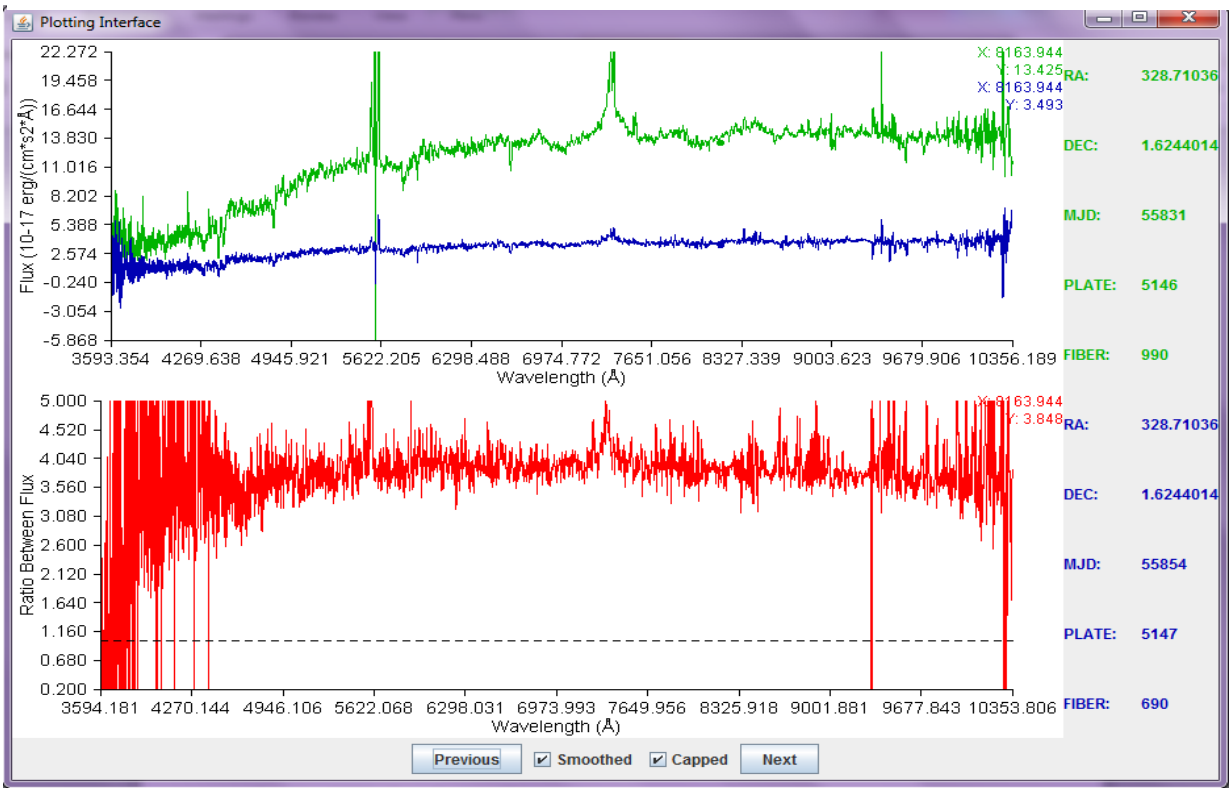

often not a serious issue. However, when much less flux is seen in one spectrum over the other for the entire spectral range, the most likely explanation is that some photons were absorbed by an obstructing medium, the most obvious of which being earth's atmosphere. The bottom comparison in Figure 11 shows a potential example of this phenomenon. The general shapes of both spectra in this comparison are the same (and depict a galaxy), including the emission and absorption features. However, there is clearly much less flux in one over the other. However this is not the only anomaly seen in this comparison.

Despite the impact of atmospheric conditions on the bottom picture of Figure 11 (matching spectra are 55831-5146-990 and 55854-5147-690), there is still one anomaly well worth mentioning. At around 7350 Å, a rather distinct peak can be seen in both spectra. This emission feature is quite odd for a galaxy, and because it appears in both spectra, is likely not the cause of atmospheric interference. The placement of this peak is right about where it should be to represent the presence of Hβ emission in an active galaxy. The exact nature of this object can therefore not be ascertained with certainty. One of the most likely explanations is that this galaxy is about to start accreting (becoming a quasar), or has just stopped accreting, with this emission being some of its last. This is certainly an object of interest and should be revisited in later research.

Another object of interest is found in Figure 12 (matching spectra are: 55831-5146-113 and 55854-5147-465). Here, the Ly-α emission line also contains an absorption feature. If something in space or some earth-based atmospheric condition absorbed the missing photons, then they would have lost energy (as they traveled away from the host galaxy) before being absorbed, which would shift the absorption feature further away from the emission feature in the spectrum. That is not the case for this object, implying that the host galaxy absorbed some of the photons before they could escape. In essence, features like these describe clouds of gas surrounding the accretion disc (in this case primarily made up of hydrogen), and may have some relation to the torus.

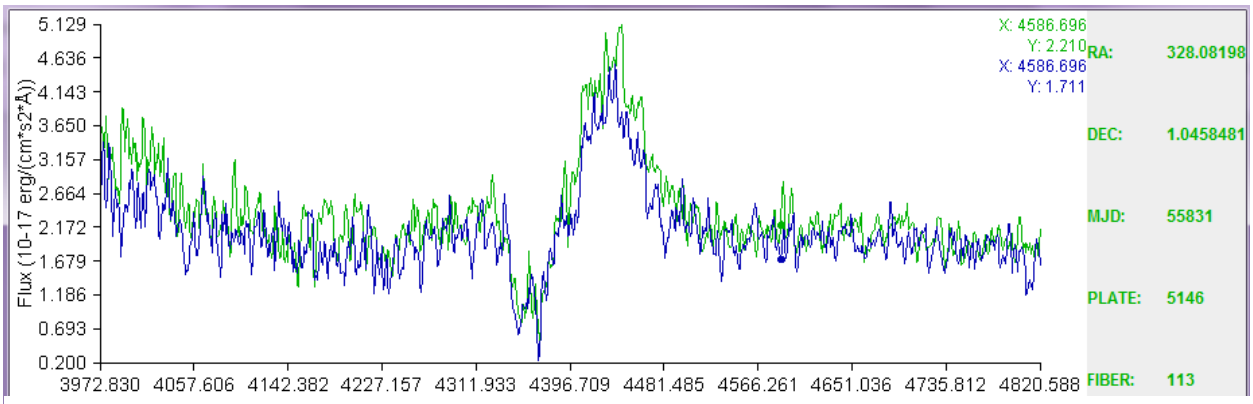

Figure 12

This is a zoomed in picture of the Ly-α line of a quasar. Because there is an absorption feature (the trough) located so close to an emission feature (the crest), it is very likely that clouds of dust (made up of mostly hydrogen) in the host galaxy have absorbed some of the emitted photons before they could escape the host galaxy.

Another anomaly found in this preliminary analysis demonstrates potential changes in the broadness of key emission lines. Figure 13 displays a quasar's Ly-α emission feature for a particular comparison (matches are 55831-5146-898 and 55854-5147-532) as well as the zoomed out picture of the entire spectrum. The overall consistency of these spectra makes it much harder to explain away the anomaly with calibration or atmospheric issues, and so is compelling reason to believe that this anomaly informs about the time-evolution of the quasar. There are two key observations about this anomaly: in one spectrum, there are fewer photons overall, as indicated by the reduced flux throughout this region;

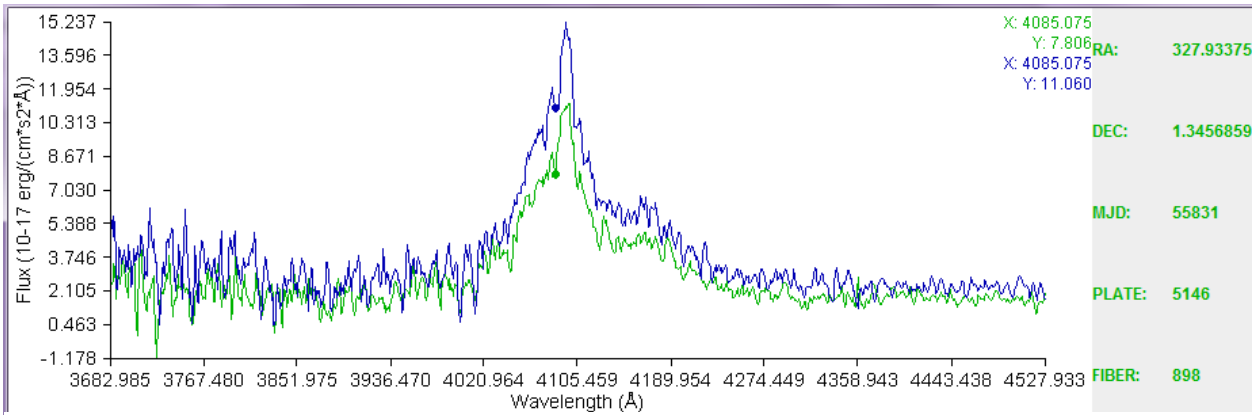

Figure 13

Above is a zoomed-in view of the Ly-α emission feature of this quasar. In one spectrum, fewer photons are emitted at this wavelength, and over a less concentrated range of wavelengths. The bottom image shows the same comparison in its entirety, to demonstrate the consistency of these measurements with one-another overall.

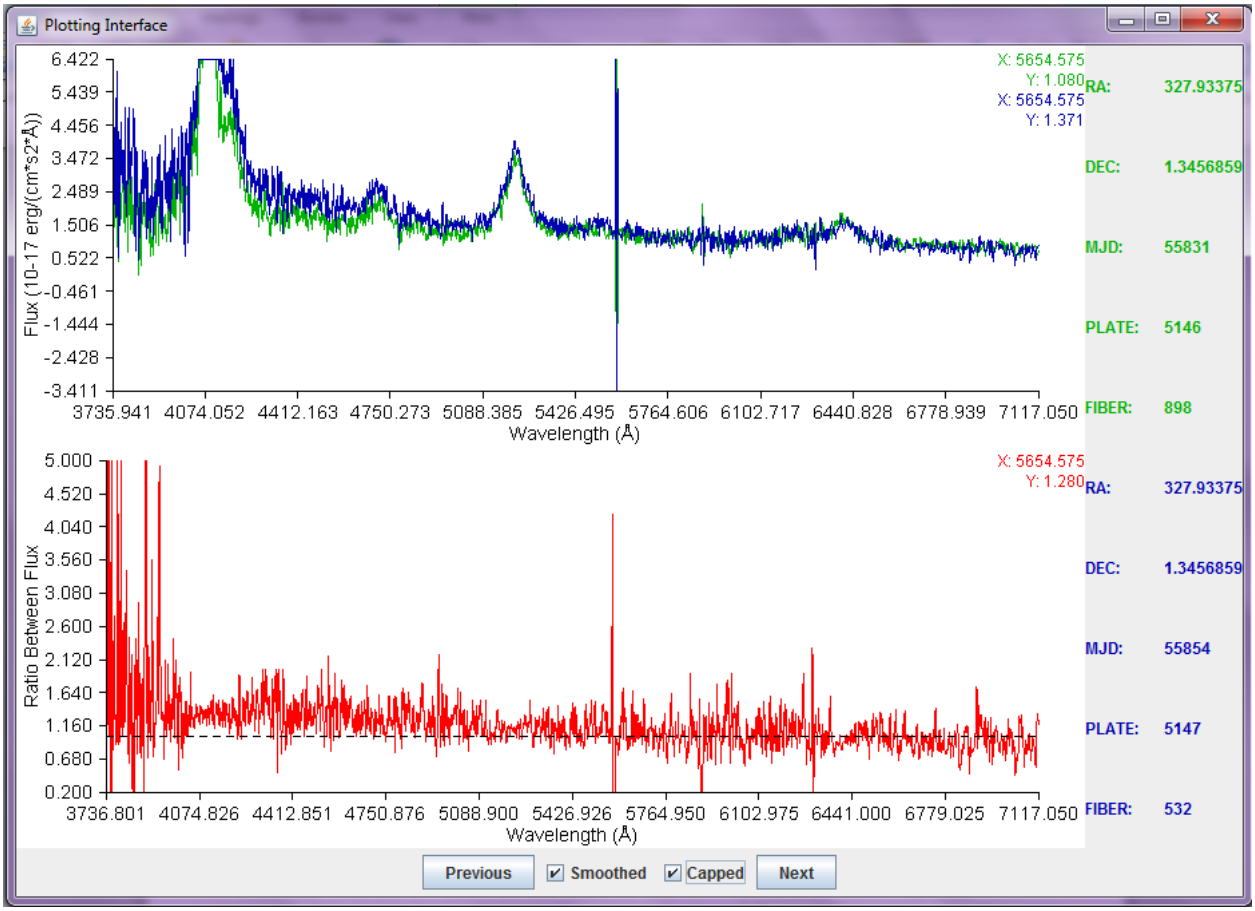

since the smaller peak appears to have the same width as the larger, the distribution of wavelengths in the smaller peak must be larger. That is to say, the photons in the larger peak are more concentrated, with the majority having a similar wavelength of around 4090 Å. So even though smaller peak appears to be just as broad as the larger, it is actually broader. The broadness of emission features could correspond with either the accretion disc velocity or obscuration in the broad line region (see Section III for full explanation). Changing broad-line features could therefore indicate a number of physical processes are occurring, the two mostly widely explore being that the torus may be discrete, allowing variable amounts of broad-line photons through depending on precise viewing angle and cloud location or the broad-line region may be accelerating or evolving in some way as not yet well understood. Both of these scenarios are explored in great detail by (Denny 2014).

Section VIII - Conclusion

This research has been extremely preliminary, and so no conclusions can yet be drawn. However, there are plenty of interesting comparisons so far, with only a small number of quasars having been reviewed. The field of quasar physics is currently in an exciting era of research, where modern observational capacity finally allows for better unification of quasar types and exploration of quasar structure. The software developed as a part of this project will certainly be a key component in future quasar research. It has certainly been a very great honor to contribute to such endeavors and it is my greatest hope that we may one day gaze across billions of light-years of space, through the miles of dusty toroidal clouds, and straight into the hearts of the most powerful and mysterious engines known to mankind.

Acknowledgements

I would like to thank Gordon Richards, PhD, and Nic Ross, PhD, for their guidance in selecting and planning this project. I would like to acknowledge Leland Machen for his contributions to the application development process. Also, I would like to acknowledge the NASA SDSS team and the ADS database system for their continued meticulous work in storing useful astronomical data and research.

References

Abazajian et al. “The Seventh Data Release of the Sloan Digital Sky Survey.” The Astrophysical Journal Supplement. Volume 182, Issue 2 (2009): article id. 543-558. <http://adsabs.harvard.edu/abs/2009ApJS..182..543A>.

Blandford, R.D. and M.J. Rees. “A ‘Twin-Exhaust’ Model for Double Radio Sources.” Monthly Notices of the Royal Astronomical Society: Volume 169, (1974). < http://articles.adsabs.harvard.edu/cgi-bin/nph-iarticle_query?1974MNRAS.169..395B&data_type=PDF_HIGH&whole_paper=YES&type=PRINTER&filetype=.pdf>.

Dawson et al. “The Baryon Oscillation Spectroscopic Survey of SDSS-III.” The Astronomical Journal. Volume 145, Issue 1 (2013): article id. 10, 41. <http://adsabs.harvard.edu/abs/2013AJ....145...10D>.

Denny et al. “AGN Type-Casting: MRK 590 No Longer Fits the Role.” Astrophysical Journal. Draft Version (April 2014). <http://arxiv.org/pdf/1404.4879.pdf>.

Fanidakis et al. “Constraints on black hole fuelling modes from the clustering of X-ray AGN.” Monthly Notices of the Royal Astronomical Society. (2013). <http://arxiv.org/pdf/1305.2200v1.pdf>.

Floyd et al. “The accretion disc in the quasar SDSS J0924+2019.” Monthly Notices of the Royal Astronomical Society. (2009). < http://arxiv.org/pdf/0905.2651v1.pdf>.

Murray, N. and J. Chiang. “Active Galactic Nuclei Disk Winds, Absorption Lines, and Warm Absorbers.” The Astrophysical Journal, Volume 454: (1995). <http://articles.adsabs.harvard.edu/cgi-bin/nph-iarticle_query?1995ApJ...454L.105M&data_type=PDF_HIGH&whole_paper=YES&type=PRINTER&filetype=.pdf>.

Neistein, Eyal and Hagai Netzer. “What triggers black-hole growth? Insights from star formation rates.” Monthly Notices of the Royal Astronomical Society. (2013). <http://arxiv.org/pdf/1302.1576v2.pdf>.

Nenkova et al. “AGN Dusty Tori: II. Observational Implications of Clumpiness.” The Astrophysics Journal, Volume 685, Issue 1 (2008). < http://arxiv.org/pdf/0806.0512v1.pdf>.

Nenkova et al. “Dust Emission from Active Galactic Nuclei.” The Astrophysics Journal, Volume 570, Issue 1 (2002). < http://arxiv.org/pdf/astro-ph/0202405v1.pdf>.

Paris et al. “The Sloan Digital Sky Survey quasar catalog: ninth data release.” Astronomy and Astrophysics. Volume 548, (2012): article id. A66. <http://adsabs.harvard.edu/abs/2012A%26A...548A..66P>.

Richards, Gordon T. “AGN Outflows in Emission and Absorption: The SDSS Perspective.” eprint arXiv:astro-ph/0603827. (2006). <http://adsabs.harvard.edu/abs/2006astro.ph..3827R>.

Ross et al. “The SDSS-III Baryon Oscillation Spectroscopic Survey: Quasar Target Selection for Data Release Nine.” The Astrophysical Journal Supplement. Volume 199, Issue 3 (2012). <http://m.iopscience.iop.org/0067-0049/199/1/3>.

Schneider et al. “The Sloan Digital Sky Survey Quasar Catalog. V. Seventh Data Release.” The Astronomical Journal. Volume 139, Issue 6 (2010): article id. 2360. <http://adsabs.harvard.edu/abs/2010AJ....139.2360S>.

Shakura, N.I. and R.A. Sunyaev. “Black Holes in Binary Systems. Observational Appearance.” Astronomy and Astrophysics. Volume 24, (1973). < http://articles.adsabs.harvard.edu/cgi-bin/nph-iarticle_query?db_key=AST&bibcode=1973A%26A....24..337S&letter=.&classic=YES&defaultprint=YES&whole_paper=YES&page=337&epage=337&send=Send+PDF&filetype=.pdf>.

Sikora et al. “Radio-Loudness of Active Galactic Nuclei: Observational Facts and Theoretical Implications.” eprint arXin:astro-ph/0604095. (2007). < http://www.slac.stanford.edu/cgi-wrap/getdoc/slac-pub-12284.pdf>.

Stoughton et al. “Sloan Digital Sky Survey: Early Data Release.” The Astronomical Journal. Volume 123, Issue 1 (2002): pp. 485-548. <http://adsabs.harvard.edu/abs/2002AJ....123..485S>.

“Types of Astronomical Spectra.” Australia Telescope National Facility. CSIRO. Web. 16 May 2013. <http://www.atnf.csiro.au/outreach/education/senior/astrophysics/spectra_astro_types.html>.

Thomsen, D.E. “End of the World: You Won’t Feel a Thing.” Society for Science & the Public: Volume 131, Issue 25 (1987). <http://www.jstor.org/stable/i380987>.

Urry, Megan and Paolo Podovani. “Unified Schemes for Radio-Loud Active Galactic Nuclei.” Publications of the Astronomical Society of the Pacific. Volume 107, (1995): p. 803. <http://adsabs.harvard.edu/abs/1995PASP..107..803U>.

Appendix I – Source Code Excerpts

This appendix contains highlights of Spectrum Analysis Software, specifically bits of code which serve particularly interesting or scientific functions. Each is accompanied by a brief explanation (in blue) and labeled with its java source file.

Excerpt 1: from TableElement.java

```
/**
 * Returns true if two table elements fall within 2.0 arcseconds of each other.
 */
public Boolean isMatch(TableElement that) {
	double r1 = this.getCoords()[0] * Math.cos(this.getCoords()[1]
							* Math.PI / 180);
	double r2 = that.getCoords()[0] * Math.cos(that.getCoords()[1]
							* Math.PI / 180);
	double d1 = this.getCoords()[1];
	double d2 = that.getCoords()[1];

	double angularDistance = Math.sqrt( (r1-r2)*(r1-r2) + (d1-d2)*(d1-d2) )*3600;
								// in arcsecs

	if( angularDistance <= Configurations.ANGULAR_DISTANCE_THRESHOLD)
		return true;
	else
		return false;
}
```

Excerpt 2: from FileManager.java

```
/**
 * Updates the table specified in Configurations.java by checking
 * which files are in the "downloads/" directory. Sets statuses
 * in real time to reflect current stage of process. Compares
 * downloaded files to find matches and updates the table with
 * this information as well. Backup table is created beforehand.
 *
 * @throws IOException
 */
public void updateTable() throws IOException {
	String backup = makeBackupTable();
	ArrayList<TableElement> table = new ArrayList<TableElement>();
	try {
		setStatus(Status.READING);
		File pwd = new File(WORKING_DIRECTORY.toString());
		for (File current : pwd.listFiles()) {
			setFile(current.getName());
			TableElement temp = TableElement.ParseFitFile(current);
			if(temp != null)
				table.add( temp );
		}
		setFile("");
		setStatus(Status.SORTING);
		Collections.sort(table);
		for(int i = 0; i < table.size(); i++)
```

```
                table.get(i).setUniqueID(i);
            setStatus(Status.MATCHING);
            for(int i = 0; i < table.size(); i++) {
                TableElement tei = table.get(i);
                setFile(tei.getFilename());
                for(int j = i + 1; j < table.size(); j++) {
                    TableElement tej = table.get(j);
                    if( tei.isMatch(tej) ) {
                        tei.addMatch(tej);
                        tej.addMatch(tei);
                    }
                }
            }
            setFile("");
            setStatus(Status.WRITING);
            writeTable(table);
            remove(backup);
        } catch (Exception e) {
            restoreBackupTable(backup);
            throw (new IOException("ERROR: Table IOS failed.", e));
        }
}
```

Excerpt 3: from TableManager.java

```
import nom.tam.fits.*;
/**
 * Opens a fits file, retrieves information regarding plate and position,
 * and returns a TableElement initialized with these details. There are
 * different labels for RA and Dec between data releases, and these are
 * retrieved from SDSS.java.
 * information.
 */
public static TableElement ParseFitFile(File uneditedFileURL) throws IOException {
        // remove the URL to get just the filename //
        String filename = uneditedFileURL.getName();

        // then read in the fits file and extract the plate and coordinate information
            from the header //
        TableElement element = new TableElement(filename);

        try {
            Fits fitFileImport = new Fits( new File(
                    WorkingDirectory.DOWNLOADS.toString(), filename ) );
            Header header = fitFileImport.getHDU( 0 ).getHeader();

            double[] coords = { 0, 0 };
            int[] plateInfo = { 0, 0, 0 };

            // These header labels need to be read in this order only  //
            // so that the data can be stored in the table accurately. //
            // coords={RAOBJ,DECOBJ}; plateInfo={MJD,PLATEID,FIBERID}  //
            plateInfo[0] = header.getIntValue("MJD");
            plateInfo[1] = header.getIntValue("PLATEID");
```

```
                plateInfo[2] = header.getIntValue("FIBERID");

                // Must set plate info before looking up coords so that _release is
                      initialized //
                element.setPlateInfo(plateInfo);

                coords[0] = header.getDoubleValue(_release.RA_HEADER);
                coords[1] = header.getDoubleValue(_release.DEC_HEADER);
                element.setCoords(coords);

                fitFileImport.getStream().close();

          } catch ( Exception e ) {
                ErrorLogger.update( "Could not load file: " + filename, e );
                element = null;
          }

          return element;
}
```

Excerpt 4: from TableManager.java

```
/**
 * Opens a fits file, retrieves the two necessary coefficients and
 * flux data, calculates the necesary x-axis information, and
 * stores all of this as member variables of the class (updating itself).
 */
public void initializeSpectrum() {
 try {
       Fits fitFileImport = new Fits( new File(
                   WorkingDirectory.DOWNLOADS.toString(), getFilename() ) );
       Header header = fitFileImport.getHDU( 0 ).getHeader();

       // read these two coefficients from the header
       double c0 = header.getDoubleValue( "COEFF0" );
       double c1 = header.getDoubleValue( "COEFF1" );

       float[] dataX, dataY;

       // read in the flux data
       dataY = _release.getDataY(fitFileImport);

       // generate the wavelength data
       dataX = new float[dataY.length];
       for ( int i = 0; i < dataX.length; i++ )
             dataX[i] = (float) Math.pow( 10, ( c0 + c1 * i ) );
       setSpectrumData( dataX, dataY );

       fitFileImport.getStream().close();
 } catch (Exception e) {
       ErrorLogger.update( "Could not load file: " + getFilename(), e );
 }
}
```

Excerpt 5: from SDSS.java

```
/**
 * This takes an already successfully opened fit(s) file and
 * retrieves the flux information stored there. This method
 * depends on the release (and may need to be updated for
 * future releases).
 */
public float[] getDataY(Fits fitFileImport) throws Exception {
	float[] dataY = null;
	BasicHDU spectralDataHeader;

	switch(this) {
	case one_two:
		spectralDataHeader = fitFileImport.getHDU( 0 );
		dataY = ( (float[][]) spectralDataHeader.getData().getData() )[0];
		break;
	case three:
		spectralDataHeader = fitFileImport.getHDU( 1 );
		dataY = (float[]) ( (TableHDU) spectralDataHeader ).getColumn( 0 );
		break;
	}

	return dataY;
}
```

Excerpt 6: from SDSS.java

```
/**
 * Takes in MJD, plate, fiber and returns the formatted URL as needed for
 * downloading files from SDSS. This method depends on the release (and
 * will need to be updated for future releases).
 */
public String formatUrl(int[] plateInfo) {
	/*
	 * Example of fully formatted URL is:
	 * http://das.sdss.org/spectro/1d_26/1615/1d/spSpec-53166-1615-513.fit
	 * Where MJD = 53166, plate = 1615, and fiber = 513
	 * Fiber needs to have padded 0s if less than 100 and 1000
	 */
	String fiberStr = "", str = "";
	int mjd = plateInfo[0], plate = plateInfo[1], fiber = plateInfo[2];

	switch(this) {
	case one_two:
	    fiberStr = String.format("%03d", fiber);
	    str = "http://das.sdss.org/spectro/1d_26/" + plate + "/1d/spSpec-"
	          + mjd + "-" + plate + "-" + fiberStr + ".fit";
	    break;
	case three:
	    fiberStr = String.format("%04d", fiber);
	    str = "http://data.sdss3.org/sas/dr10/boss/spectro/redux/v5_5_12/spectra/"
	          + plate + "/spec-" + plate + "-" + mjd + "-" + fiberStr + ".fits";
	    break;
	}
```

```
	return str;
}
```

Excerpt 7: from FileManager.java

```
/**
 * Uses an HttpUrlConnection to access URLs as specified in previous
 * methods (and stored as a member of this class) and downloads them
 * to the working directory specified as a member of this class. If a
 * file already exists in that directory, then it overwrites it.
 *
 * @throws IOException
 */
public Boolean download() throws IOException {
 try {
	ExecutorService pool = Executors.newFixedThreadPool(30);
	for (final String str : _downloadUrls) {
		pool.submit(new Runnable() {
			@Override
			public void run() {
			 try {
				File destination = new File(WORKING_DIRECTORY.toString(),
					str.substring(str.lastIndexOf("/") + 1));

				URL url = new URL(str);
				HttpURLConnection connect =
					(HttpURLConnection) url.openConnection();
				Files.copy(connect.getInputStream(),
					destination.toPath(),
					StandardCopyOption.REPLACE_EXISTING);
				connect.disconnect();
			 } catch (Exception e) {
				ErrorLogger.update("ERROR: Can't retrieve files.", e);
			 }
			}
		});
	}
	pool.shutdown();
	pool.awaitTermination(Long.MAX_VALUE, TimeUnit.MILLISECONDS);

	return true;
 } catch ( Exception e ) {
	e.printStackTrace();
	return false;
 }
}
```

Excerpt 8: from FileManager.java

```
/**
 * Prepares for downloading files by compiling a list of URLs.
 * If a 0 is specified for the fiber number, then the entire
 * plate will be downloaded (the number of files for each release
```

```
 * is stored in SDSS.java). This method is the main interface for
 * downloading files, updating the table, and communicating these
 * updates to the display.
 *
 * @param plateInfos
 *                  - a list of all mjd,plate,fiber which needs downloading
 */
public void downloadInBackground(final ArrayList<int[]> plateInfos) {
      new SwingWorker<Void,Void>(){
            @Override
            protected Void doInBackground() throws Exception {
                  setStatus(Status.DOWNLOADING);

                  // Establishes download list //
                  for(int[] current : plateInfos) {
                        SDSS release = SDSS.getInstance(current);

                        // Checks if fiber = 0, then download entire plate //
                        if(current[2] == 0) {
                              int tmp[] = new int[3];
                              tmp[0] = current[0];
                              tmp[1] = current[1];

                              for(int i = 0; i <= release.FIBERS; i++) {
                                    tmp[2] = i;
                                    _downloadUrls.add(release.formatUrl(tmp));
                              }
                        } else
                              _downloadUrls.add(release.formatUrl(current));
                        }

                  download();
                  updateTable();
                  Main.setData( importTable() );
                  setStatus(Status.IDLE);
                  return null;
            }
      }.execute();
}
```

Excerpt 9: from QuasarSpectraTable.qst

```
## uniqueID   filename   RA,Dec   MJD,Plate,Fiber   matches ##
0       spSpec-53169-1616-100.fit       189.41984,11.586058   53169,1616,100       none
1       spSpec-53847-2235-100.fit       188.32595,26.351204   53847,2235,100       368
2       spSpec-53729-2236-100.fit       190.07586,26.572944   53729,2236,100       none
3       spSpec-53166-1615-101.fit       187.60037,11.642371   53166,1615,101       none
4       spSpec-53169-1616-101.fit       189.66829,11.932112   53169,1616,101       244,1025
(etc)
```

Appendix II – User Documentation

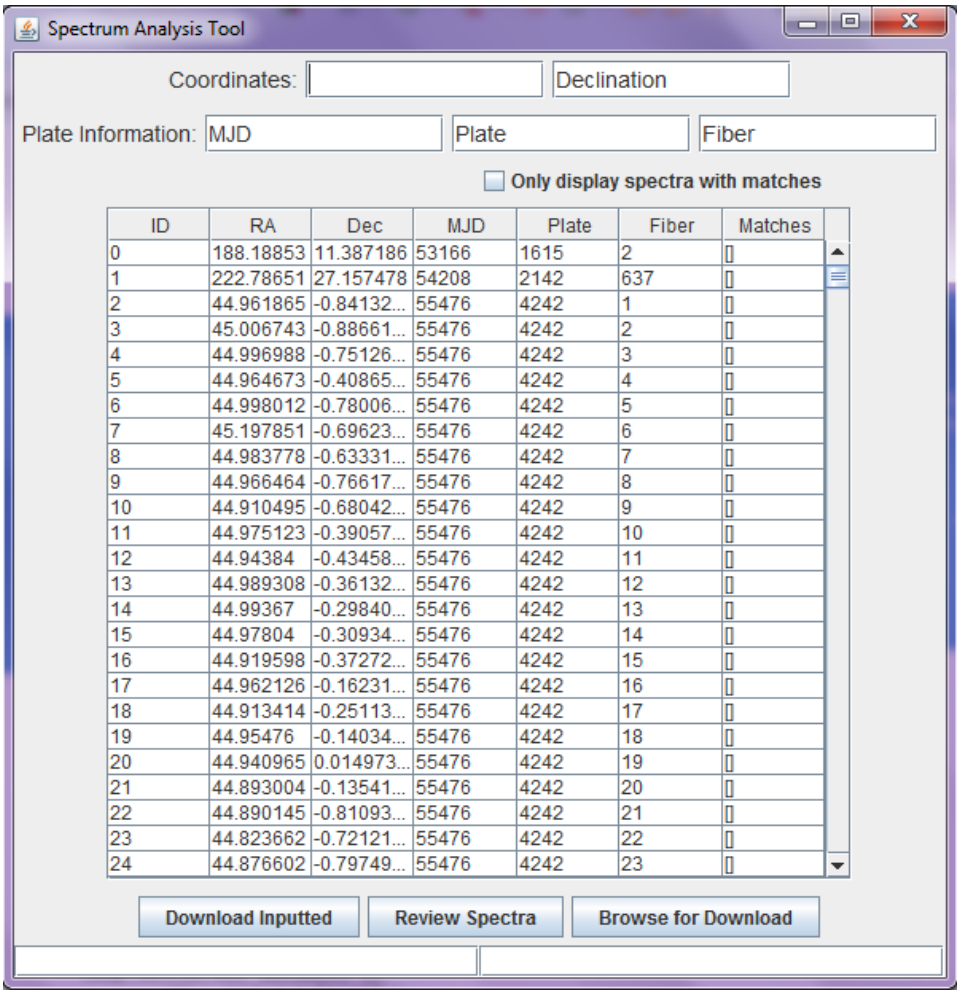

ID	RA	Dec	MJD	Plate	Fiber	Matches
0	188.18853	11.387186	53166	1615	2	[]
1	222.78651	27.157478	54208	2142	637	[]
2	44.961865	-0.84132...	55476	4242	1	[]
3	45.006743	-0.88661...	55476	4242	2	[]
4	44.996988	-0.75126...	55476	4242	3	[]
5	44.964673	-0.40865...	55476	4242	4	[]
6	44.998012	-0.78006...	55476	4242	5	[]
7	45.197851	-0.69623...	55476	4242	6	[]
8	44.983778	-0.63331...	55476	4242	7	[]
9	44.966464	-0.76617...	55476	4242	8	[]
10	44.910495	-0.68042...	55476	4242	9	[]
11	44.975123	-0.39057...	55476	4242	10	[]
12	44.94384	-0.43458...	55476	4242	11	[]
13	44.989308	-0.36132...	55476	4242	12	[]
14	44.99367	-0.29840...	55476	4242	13	[]
15	44.97804	-0.30934...	55476	4242	14	[]
16	44.919598	-0.37272...	55476	4242	15	[]
17	44.962126	-0.16231...	55476	4242	16	[]
18	44.913414	-0.25113...	55476	4242	17	[]
19	44.95476	-0.14034...	55476	4242	18	[]
20	44.940965	0.014973...	55476	4242	19	[]
21	44.893004	-0.13541...	55476	4242	20	[]
22	44.890145	-0.81093...	55476	4242	21	[]
23	44.823662	-0.72121...	55476	4242	22	[]
24	44.876602	-0.79749...	55476	4242	23	[]

Figure 14
The main display of the application, with nothing yet being filtered.

The source code is located in an online repository which still requires formatting before being made public. The developer documentation will be located there once it is completed (before the end of this term). The following user documentation is meant to be a guide on how-to use the software, explaining all of the features and what they mean in detail.

The application will be runnable via GUI or command line by simply activating the Java Archive ("AnalysisTool.jar"). This software is cross-platform and should run on any OS and environment, although Java will likely need to be installed and up-to-date (details on this will follow once cross-platform testing is completed).

Once the application is activated for the first time, it will check if any files have been downloaded in order to initialize the display, and create an empty table if nothing is found. Subsequent operation of the application will not perform this check assuming the table can be found and read. The table is a text file which contains information regarding all of the downloads on the machine and their match information (i.e. which files describe the same objects as one another). Its extension is "qst" for disambiguation. The table is updated after each download or if it is corrupted, and will verify what is currently downloaded on the machine every time it updates.

The main screen consists of several search bars and a list of downloaded files (see Figure 14).The list of files can be sorted by typing information into the search bar, by choosing the option which only displays files with matches, or both (Figure 15).

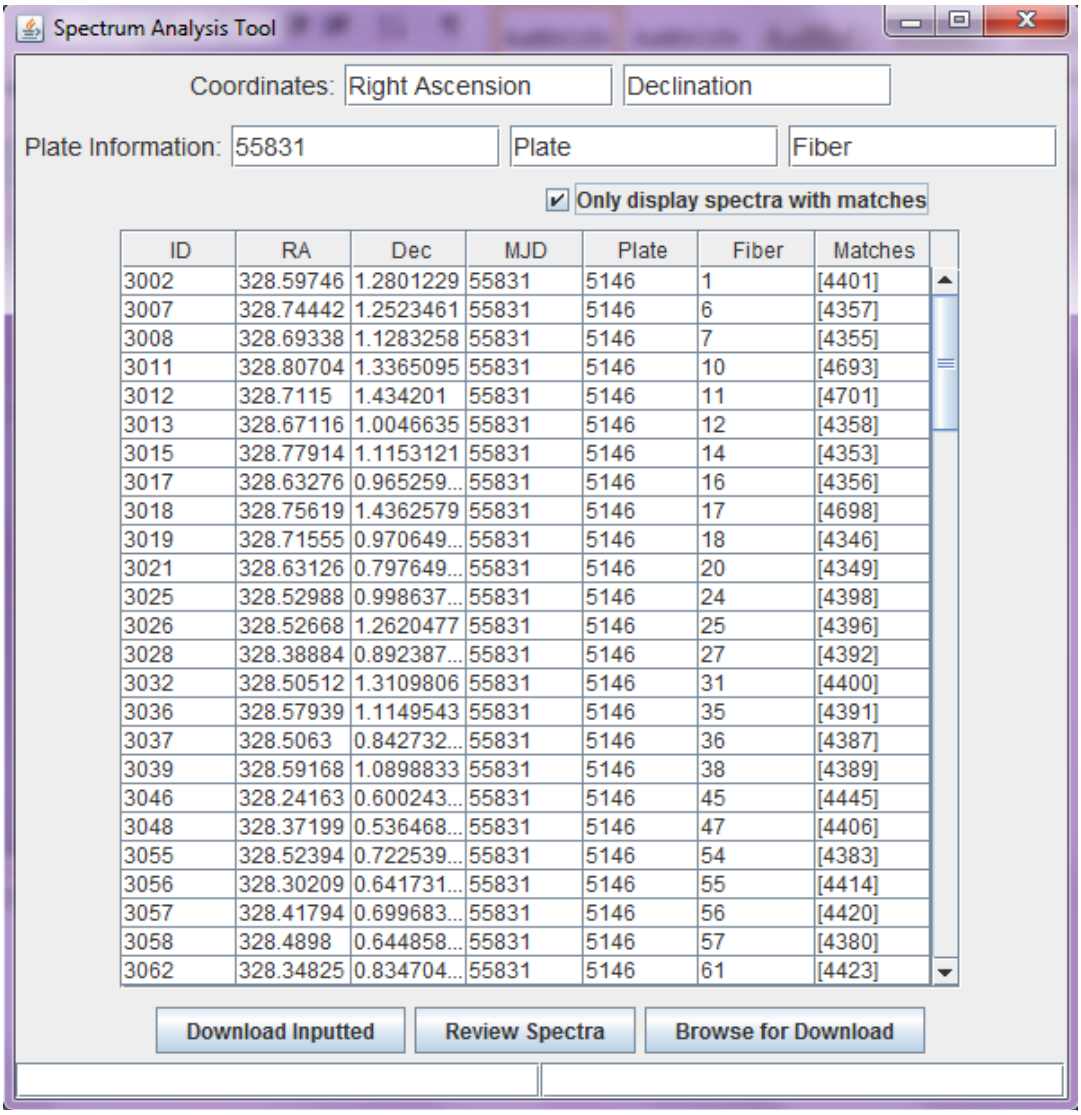

ID	RA	Dec	MJD	Plate	Fiber	Matches
3002	328.59746	1.2801229	55831	5146	1	[4401]
3007	328.74442	1.2523461	55831	5146	6	[4357]
3008	328.69338	1.1283258	55831	5146	7	[4355]
3011	328.80704	1.3365095	55831	5146	10	[4693]
3012	328.7115	1.434201	55831	5146	11	[4701]
3013	328.67116	1.0046635	55831	5146	12	[4358]
3015	328.77914	1.1153121	55831	5146	14	[4353]
3017	328.63276	0.965259...	55831	5146	16	[4356]
3018	328.75619	1.4362579	55831	5146	17	[4698]
3019	328.71555	0.970649...	55831	5146	18	[4346]
3021	328.63126	0.797649...	55831	5146	20	[4349]
3025	328.52988	0.998637...	55831	5146	24	[4398]
3026	328.52668	1.2620477	55831	5146	25	[4396]
3028	328.38884	0.892387...	55831	5146	27	[4392]
3032	328.50512	1.3109806	55831	5146	31	[4400]
3036	328.57939	1.1149543	55831	5146	35	[4391]
3037	328.5063	0.842732...	55831	5146	36	[4387]
3039	328.59168	1.0898833	55831	5146	38	[4389]
3046	328.24163	0.600243...	55831	5146	45	[4445]
3048	328.37199	0.536468...	55831	5146	47	[4406]
3055	328.52394	0.722539...	55831	5146	54	[4383]
3056	328.30209	0.641731...	55831	5146	55	[4414]
3057	328.41794	0.699683...	55831	5146	56	[4420]
3058	328.4898	0.644858...	55831	5146	57	[4380]
3062	328.34825	0.834704...	55831	5146	61	[4423]

Figure 15
The list filtered by both MJD and matches-only. Notice how every list item has an MJD of 55831, and a match listed in the last column. The numbers in that column contain the Unique IDs of all (if any) of that element's matches.

If there is no file in the list corresponding to an inputting MJD, Plate, or Fiber, then it can be downloaded by clicking the "Download Inputted" button at the button of the screen. Objects cannot be located on the SDSS website if only the RA and Dec are provided at this time. If a user would like to download a single fit file, then they must supply all three bits of plate information (an MJD, plate, and fiber number). However, if a user would like to download an entire plate's worth of fibers, then they need only provide an MJD and plate number. Inputting a 0 or leaving the fiber textbox blank will automatically download the entire plate. If incorrect data is entered, then the UI will display an error letting the user know what part went wrong (Figure 16).

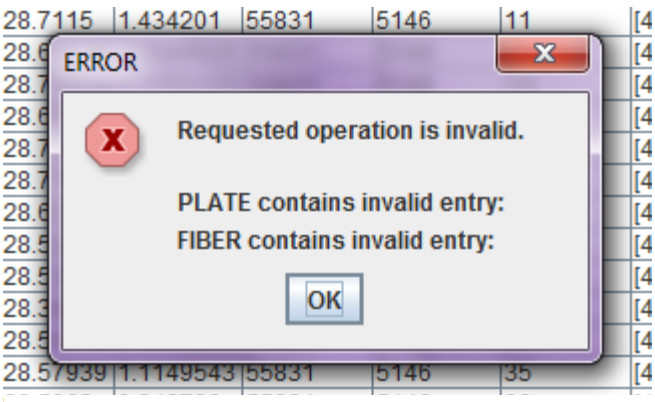

Figure 16
Display which lets a user know which input was invalid. Here is says leaving Fiber blank is invalid, but this bug in the error message will be fixed shortly.

Downloads can also be initiated by clicking the other button, "Browse for Download." This will allow the user to open a text file with a list of

MJD,plate,fiber information. This file must be formatted particularly in order to work, with no header, each set of information listed one per line, comma delimited, and with no spaces. The file should have the extension "txt" and as before, if the fiber information is omitted or listed as 0 for any given set of plate information, then the entire plate will be downloaded (See Figure 17 for an example).

```
1 53166,1615,2
2 53169,1616
3 53847,2235,0
4
```

Figure 17
Excerpt from plate download file. The grey numbers are the line numbers inserted by the text editor. Any line with no fiber number specified or a fiber number of 0 will download the whole plate.

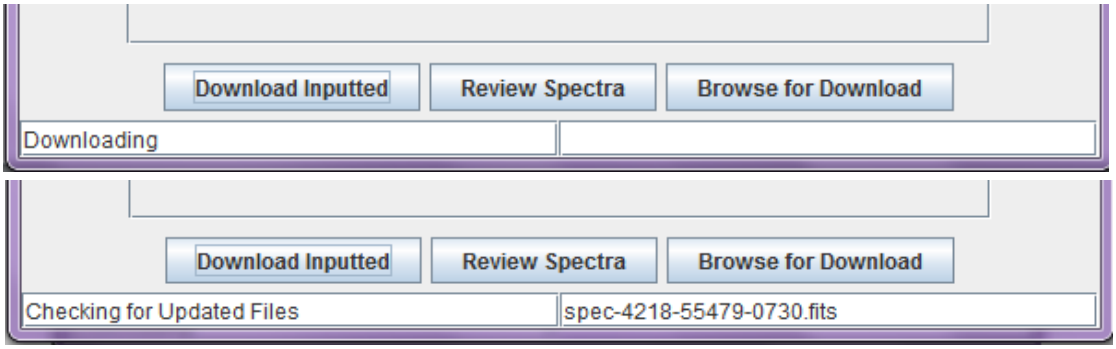

Figure 198
The bottom bar lets the user know what is currently happening in the download process. Downloading means retrieving files from the internet, and checking for updates means importing each downloaded file and comparing it for matches. Other statuses include idle (when it is done), sorting table, and writing table.

Once a download is successfully started, the bottom of the screen will update based on the current status of the download process. Figure 18 has two examples. When it is done downloading, this bar will say "Idle."

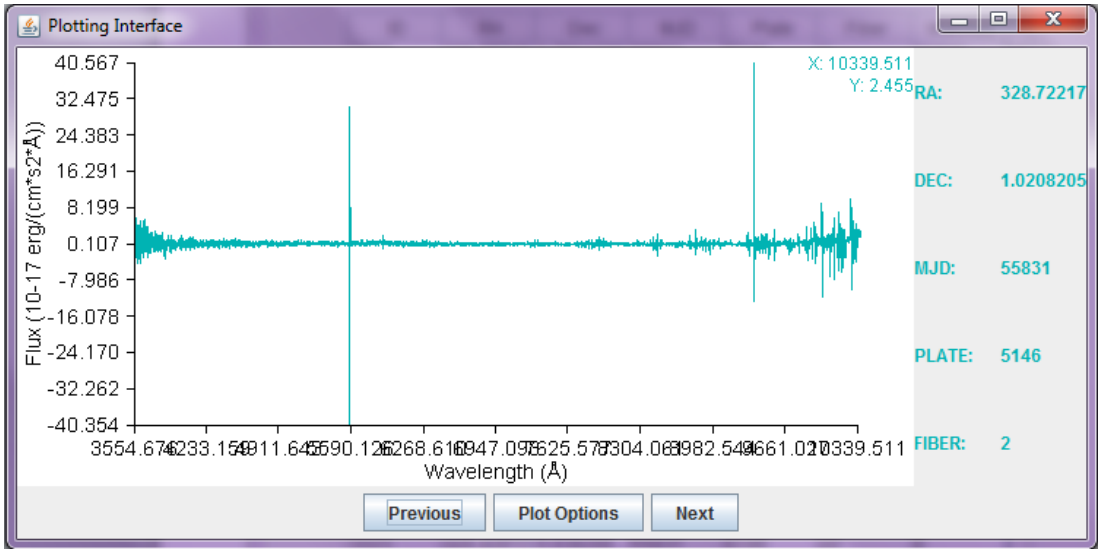

Figure 18
A single spectrum with legend.

Once a spectrum has been selected for plotting (via clicking on an element in the list), the user can hit "Review Spectra" to bring up the plotting interface. If there are multiple matches for this spectra, then all of them will be plotted at once. Likewise, if there is only one match, this individual spectrum will be plotted alone. If there are exactly two matches, then the plotting interface will automatically calculate the ratio and display that as well in its own plot. See Figure 19 for the layout of this interface. The features of this interface include zoom and panning options (Figure 20), as well as a plot options UI. The plot options screen (Figure 21) allows the user to select which matches to plot (if there are more than one), including the ability to plot one at a time. Any time two spectra are selected, the ratio will automatically be calculated. The other plot options are to

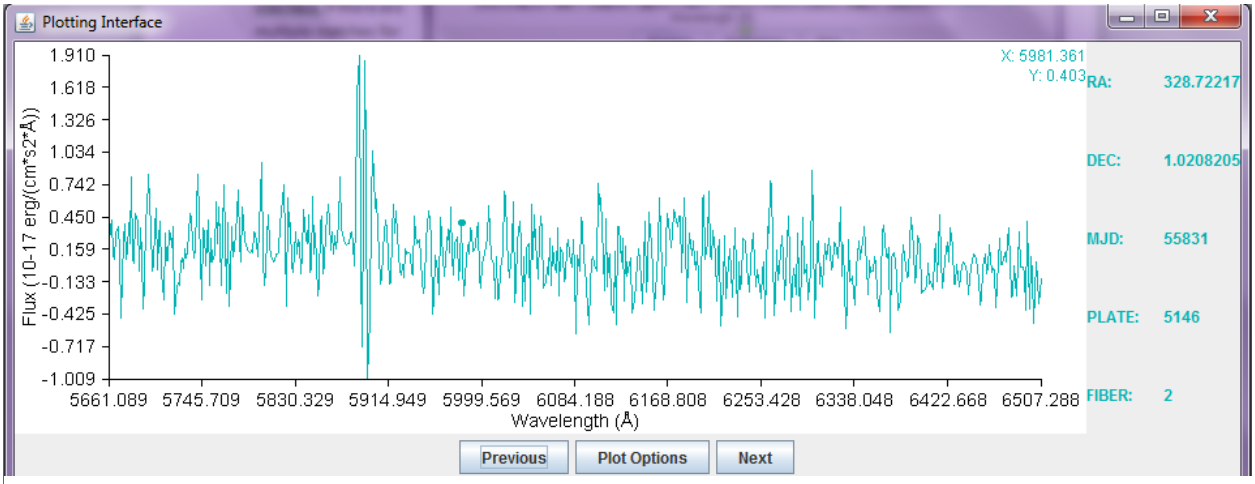

Figure 20
Zoomed-in version of spectrum from Figure 19.

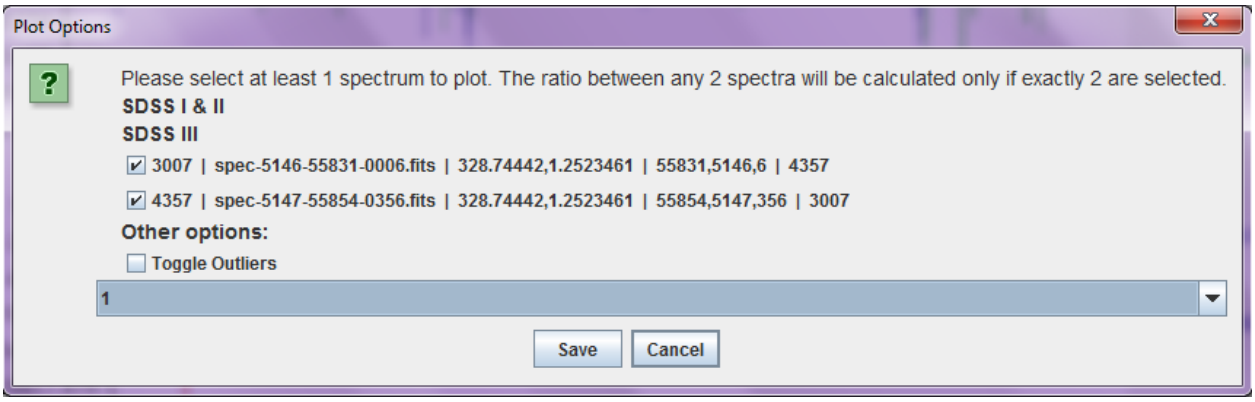

Figure 21
Plot Options menu, with the two match options listed under what release they are from, the toggle extreme outliers checkbox, and the drop-down box for the smoothing radius.

select a smoothing radius and to remove the extreme flux values from view. The smoothing feature will average over the number of pixels specified by the radius and the toggle for removing extremities will remove all extraordinarily large Y values from the main plot, as well as limit the ratio to a range of 0.2 – 5. The smoothing radius, extremity cap setting, and zoom/pan features will all persist onto the next plot if one would like to quickly review a particular part of the spectrum on all spectra with matches.

Flipping between spectra with matches is the purpose of the previous and next buttons. These will intelligently search for the next downloaded spectrum with matches and display it and all of its matches. If it reaches the end of the list without finding a match, then it will start at the beginning and search up to where the user is currently. An error message will appear if there aren't any spectra with matches. Even if the user toggles off the currently displayed spectra, it will still be kept track of as current. The search for the next comparison uses whatever the initially selected spectra was and ignores duplicates caused by low indexed matches lining up with high index matches. In other words, previous and next will only find comparisons that haven't yet been viewed by the user no matter where they start in the list or in which direction they'd like to flip. This provides a powerful framework for reviewing and comparing many spectra at once, with as much precision as the user would like.